Elucidation of the 14-3-3ζ interactome reveals critical roles of RNA-splicing factors during adipogenesis

Received for publication, September 6, 2017, and in revised form, March 5, 2018 Published, Papers in Press, March 12, 2018, DOI 10.1074/jbc.M117.816272

Yves Mugabo[‡§], **Mina Sadeghi**[‡§], **Nancy N. Fang**[¶1], **Thibault Mayor**[¶], **and Gareth E. Lim**[‡§2]

From the [‡]*Centre Hospitalier de l'Université de Montréal, Montréal, Québec H2X 029, Canada, the* [§]*Department of Medicine, Université de Montréal, Montréal, Québec H3T 1J4, Canada, and the* [¶]*Department of Biochemistry and Molecular Biology, University of British Columbia, Vancouver, British Columbia V6T 1Z4, Canada*

Edited by Ronald C. Wek

Adipogenesis involves a complex signaling network requiring strict temporal and spatial organization of effector molecules. Molecular scaffolds, such as 14-3-3 proteins, facilitate such organization, and we have previously identified 14-3-3ζ as an essential scaffold in adipocyte differentiation. The interactome of 14-3-3ζ is large and diverse, and it is possible that novel adipogenic factors may be present within it, but this possibility has not yet been tested. Herein, we generated mouse embryonic fibroblasts from mice overexpressing a tandem affinity purification (TAP) epitope–tagged 14-3-3ζ molecule. After inducing adipogenesis, TAP–14-3-3ζ complexes were purified, followed by MS analysis to determine the 14-3-3ζ interactome. We observed more than 100 proteins that were unique to adipocyte differentiation, 56 of which were novel interacting partners. Among these, we were able to identify previously established regulators of adipogenesis (*i.e.* Ptrf/Cavin1) within the 14-3-3ζ interactome, confirming the utility of this approach to detect adipogenic factors. We found that proteins related to RNA metabolism, processing, and splicing were enriched in the interactome. Analysis of transcriptomic data revealed that 14-3-3ζ depletion in 3T3-L1 cells affected alternative splicing of mRNA during adipocyte differentiation. siRNA-mediated depletion of RNA-splicing factors within the 14-3-3ζ interactome, that is, of Hnrpf, Hnrpk, Ddx6, and Sfpq, revealed that they have essential roles in adipogenesis and in the alternative splicing of *Pparg* and the adipogenesis-associated gene *Lpin1*. In summary, we have identified novel adipogenic factors within the 14-3-3ζ interactome. Further characterization of additional proteins within the 14-3-3ζ interactome may help identify novel targets to block obesity-associated expansion of adipose tissues.

Central to the development of obesity are the increases in number and size of adipocytes, according to nutrient availability (1, 2). Despite various therapies to limit weight gain and promote weight loss, it is surprising that none specifically target the adipocyte to limit its expansion or growth (1, 2). The complex transcriptional network and cellular processes that govern the differentiation of adipocyte progenitor cells contribute to the difficulty in targeting adipocytes therapeutically (1, 2). Protein phosphorylation is a key post-translational modification that determines the activation state, subcellular localization, and stability of adipogenic regulators (3–7). Furthermore, phosphorylation status also determines their interactions with molecular scaffold proteins, which aid in the coordination of complex transcriptional networks (3, 4).

We previously identified the molecular scaffold, 14-3-3ζ, as a critical regulator of glucose homeostasis and adipogenesis (4, 8, 9). Specific to the adipocyte, systemic deletion of 14-3-3ζ in mice significantly reduced visceral adiposity and impaired adipocyte differentiation, whereas transgenic overexpression of 14-3-3ζ exacerbated high-fat diet induced obesity (4). The hedgehog transcription factor, Gli3, was identified as a critical downstream effector in 14-3-3ζ–mediated adipogenesis (4), but the diversity of proteins in the 14-3-3ζ interactome suggests the possibility that other interacting proteins or pathways parallel to Gli3 may be also involved.

Unbiased approaches, such as proteomics and transcriptomics, can lead to the discovery of novel factors that drive adipogenesis, in addition to providing insight into physiological pathways influenced by adipogenic regulators like 14-3-3ζ (4, 10–13). All seven mammalian 14-3-3 isoforms have large, diverse interactomes (8, 12–15), and they are dynamic and change in response to various stimuli (10–13). Thus, inducing pre-adipocytes to differentiate may permit the identification of novel differentiation-specific factors within the 14-3-3ζ interactome and reveal pathways and biological processes that are essential to the development of a mature adipocyte.

To elucidate the 14-3-3ζ interactome during adipogenesis, we employed a proteomic-based discovery approach. Herein, we report that previously established factors required for adipogenesis, such as Ptrf/Cavin1 and Phb2 (Prohibitin-2), can be detected in the interactome, and novel factors, such as those involved in RNA splicing, are also enriched in the interactome during differentiation. To test for their roles in adipogenesis, siRNA knockdown approaches were used and revealed the requirement for RNA-splicing factors, such as Hnrpf, Sfpq, and Ddx6. Taken together, these findings demonstrate the usefulness of examining the interactome of 14-3-3 proteins in the

This work was supported by Canadian Institutes of Health Research Project Grant PJT-153144 (to G. E. L.). This work was supported in part by postdoctoral fellowships from the Juvenile Diabetes Research Foundation (JDRF) and the Canadian Diabetes Association (to G. E. L.). The authors declare that they have no conflicts of interest with the contents of this article.

This article contains Table S1 and Figs. S1–S4.

[1] Present address: Dept. of Medical Genetics, Harvard Medical School, Boston, MA 02115.

[2] To whom correspondence should be addressed: CRCHUM, Tour Viger, Rm. 08.482, 900 Rue St. Denis, Montréal, QC H2X 029, Canada. Tel.: 514-890-8000, Ext. 12927; E-mail: gareth.lim@umontreal.ca.

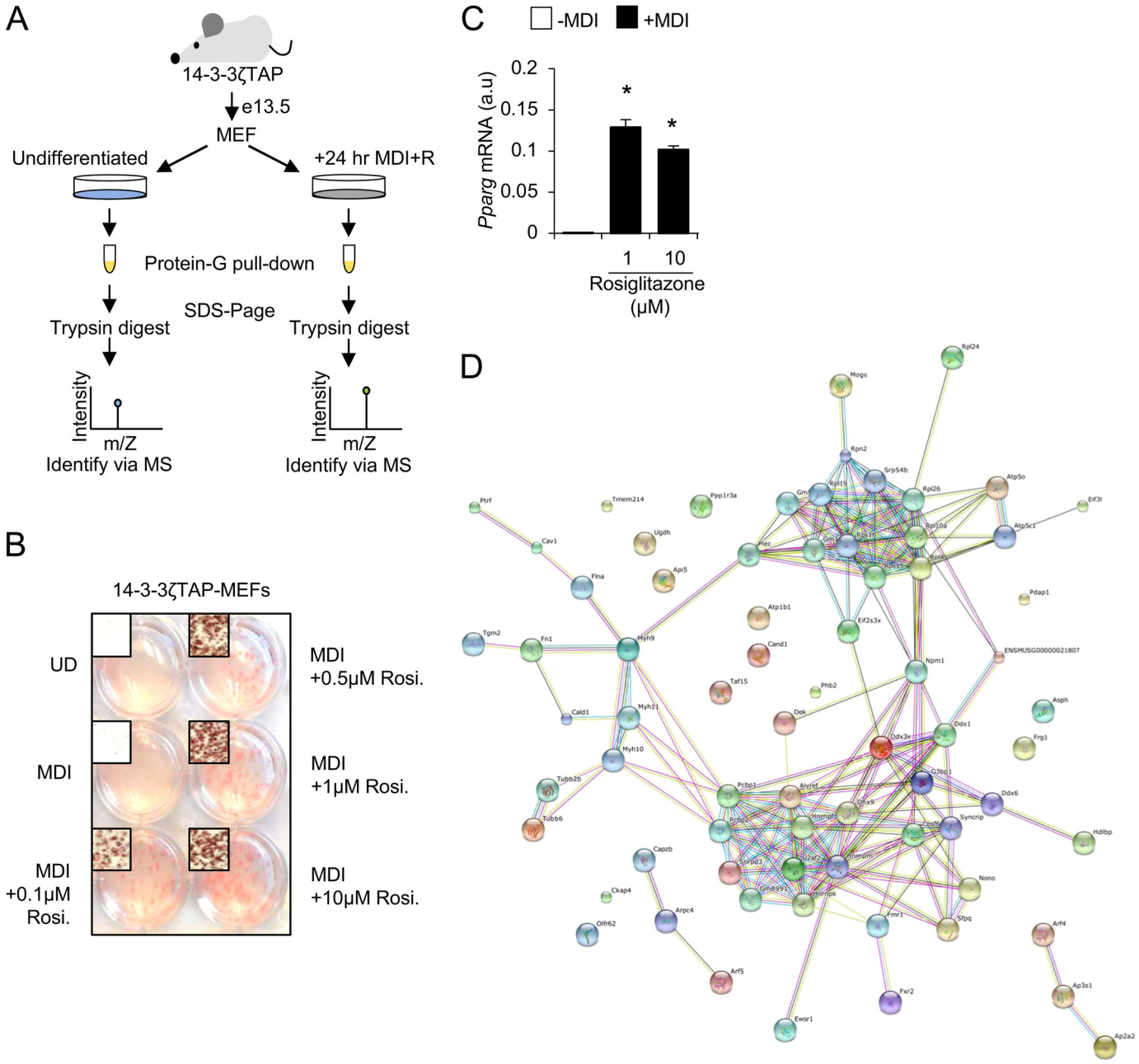

Figure 1. Generation of TAP–14-3-3ζ MEFs to elucidate the 14-3-3ζ interactome. *A*, schematic overview of generation and use of TAP–14-3-3ζ MEFs to determine the 14-3-3ζ interactome during adipogenesis. *B* and *C*, verification of TAP–14-3-3ζ MEF adipogenesis by Oil Red-O incorporation, 7 days after induction (*B*), or *Pparg* mRNA expression by quantitative PCR (*C*), 2 days following induction (*UD*, undifferentiated cells; representative of $n = 4$ independent experiments; *, $p < 0.05$ when compared with -MDI; *bar graphs* represent means ± S.D.). *Rosi.*, rosiglitazone. *D*, String-db (17) was used to visualize and cluster proteins according to their biological function, resulting in three distinct clusters: RNA splicing/processing factors, components of the ribosomal complex, and components of actin/tubulin network.

context of a physiological process, such as adipocyte differentiation, and highlight the ability to find novel functional regulators through this approach. Understanding how the interactome is influenced by disease states, such as obesity, may lead to the identification of novel proteins that contribute to disease pathogenesis.

Results

Generation of TAP–14-3-3ζ mouse embryonic fibroblasts

To examine how adipocyte differentiation influences the 14-3-3ζ interactome, we generated mouse embryonic fibroblasts (MEFs)[3] derived from transgenic mice that moderately overexpress a TAP-epitope–tagged human 14-3-3ζ molecule (TAP–14-3-3ζ) (4) (Fig. 1*A*). This approach was chosen to circumvent the variability in the expression of transiently expressed proteins and increased specificity of protein purification with epitope-tagged proteins (16). Differentiation of TAP–14-3-3ζ MEFs was induced with an established adipogenic mixture (MDI: insulin, dexamethasone, and isobutylm-

[3] The abbreviations used are: MEF, mouse embryonic fibroblast; siCon, control siRNA; TAP, tandem affinity purification.

Table 1
Proteins with at least two unique peptides with a total spectral count in differentiated cells of ≥2 in comparison to undifferentiated cells

				Total spectrum IP1		Total spectrum IP2	
Uniprot	Description	Gene name	Σ# Peptides	D	U	D	U
Q8VDD5	Myosin-9	Myh9	102	278	129	7	2
Q4FK11	Non-POU-domain-containing, octamer binding protein	Nono	16	11	1	149	7
E9QMZ5	Plectin	Plec	123	101	41	74	23
E9QPE8	Plectin	Plec	122	99	41	75	23
G5E8B8	Anastellin	Fn1	46	60	21	58	11
Q61879	Myosin-10	Myh10	68	107	41	2	1
P97855	Ras GTPase-activating protein-binding protein 1	G3bp1	20	20	6	94	45
P61979	Heterogeneous nuclear ribonucleoprotein K	Hnrnpk	16	35	10	62	29
Q9R002	Interferon-activable protein 202	Ifi202	13	4	0	45	1
B7FAU9	Filamin, α	Flna	48	65	21	3	1
Q61033	Lamina-associated polypeptide 2, isoforms α/ζ	Tmpo	19	13	3	31	1
B2RSN3	MCG1395	Tubb2b	17	33	7	23	10
Q91VR5	ATP-dependent RNA helicase DDX1	Ddx1	29	16	3	42	17
P48962	ADP/ATP translocase 1	Slc25a4	14	27	6	29	13
P51881	ADP/ATP translocase 2	Slc25a5	12	25	6	27	10
Q60865	Caprin-1	Caprin1	19	10	3	50	23
Q8BMK4	Cytoskeleton-associated protein 4	Ckap4	17	22	5	22	6
B8JJG1	Novel protein (2810405J04Rik)	Fam98a	9	8	1	30	7
Q61029	Lamina-associated polypeptide 2, isoforms β/δ/ϵ/γ	Tmpo	14	12	4	23	2
Q8VIJ6	Splicing factor, proline- and glutamine-rich	Sfpq	19	7	2	39	16
P62702	40S ribosomal protein S4, X isoform	Rps4x	15	18	5	26	11
Q3TQX5	DEA(D/H) (Asp-Glu-Ala-Asp/His) box polypeptide 3, X-linked	Ddx3x	19	14	2	26	11
Q4VA29	MCG140066	2700060E02Rik	10	9	2	23	4
P14148	60S ribosomal protein L7	Rpl7	13	19	0	6	0
Q3UMM1	Tubulin, β 6	Tubb6	13	18	2	11	2
G3UXT7	RNA-binding protein FUS (Fragment)	Fus	7	12	2	24	9
Q8VEM8	Phosphate carrier protein, mitochondrial	Slc25a3	7	13	1	16	5
E9QPE7	Myosin-11	Myh11	18	34	13	2	0
A2A547	Ribosomal protein L19	Rpl19	6	11	1	13	1
P63038	60-kDa heat shock protein, mitochondrial	Hspd1	13	14	0	13	5
D3Z6C3	Protein Gm10119	Gm10119	12	16	3	15	6
Q9DB20	ATP synthase subunit O, mitochondrial	Atp5o	11	22	7	14	7
O70475	UDP-glucose 6-dehydrogenase	Ugdh	14	17	0	5	1
A2APD4	Small nuclear ribonucleoprotein-associated protein	Snrpb	5	5	2	19	1
O70309	Integrin β5	Itgb5	14	7	2	16	1
G3UZI2	Heterogeneous nuclear ribonucleoprotein Q	Syncrip	11	9	1	16	4
D3Z6U8	Fragile X mental retardation protein 1 homolog	Fmr1	15	8	3	21	7
O35841	Apoptosis inhibitor 5	Api5	11	8	1	12	1
A4FUS1	MCG123443	Rps16	12	9	4	24	11
Q3TLH4–5	Isoform 5 of protein PRRC2C	Prrc2c	11	5	1	14	1
P14869	60S acidic ribosomal protein P0	Rplp0	8	16	5	8	2
Q8QZY1	Eukaryotic translation initiation factor 3 subunit L	Eif3l	5	7	0	8	0
P35922	Fragile X mental retardation protein 1 homolog	Fmr1	15	7	3	21	10
Q03265	ATP synthase subunit α, mitochondrial	Atp5a1	15	14	3	4	2
P63017	Heat shock cognate 71-kDa protein	Hspa8	13	9	2	12	6
P21981	Protein-glutamine γ-glutamyltransferase 2	Tgm2	8	5	0	7	0
Q80UM7	Mannosyl-oligosaccharide glucosidase	Mogs	11	3	0	13	4
P26369	Splicing factor U2AF 65-kDa subunit	U2af2	7	7	0	8	3
A2AJM8	MCG7378	Sec61b	3	3	1	9	0
P62242	40S ribosomal protein S8	Rps8	7	12	3	3	1
P54823	DEA(D/H) (Asp-Glu-Ala-Asp/His) box polypeptide 6	Ddx6	8	2	1	13	3
Q3TML6	Eukaryotic translation initiation factor 2, subunit 3, structural gene X-linked	Eif2s3x	6	7	1	8	3
P26041	Moesin	Msn	13	5	0	12	6
P62983	Ubiquitin-40S ribosomal protein S27a	Rps27a	6	5	2	13	5
P52480	Pyruvate kinase isozymes M1/M2	Pkm2	4	2	0	8	0
Q5SUT0	Ewing sarcoma breakpoint region 1	Ewsr1	5	6	1	6	1
E9Q7H5	Uncharacterized protein	Gm8991	6	3	0	10	3
Q8C2Q8	ATP synthase γ chain	Atp5c1	7	5	1	9	3
A2AMW0	Capping protein (actin filament) muscle Z-line, β	Capzb	7	13	6	3	0
P08121	Collagen α-1(III) chain	Col3a1	6	5	0	4	0
P11087-2	Isoform 2 of collagen α-1(I) chain	Col1a1	10	3	1	8	1
Q9Z2X1-2	Isoform 2 of Heterogeneous nuclear ribonucleoprotein F	Hnrnpf	3	4	1	7	1
P11499	Heat shock protein HSP 90β	Hsp90ab1	11	6	1	6	2
P28301	Protein-lysine 6-oxidase	Lox	4	2	1	9	1
Q8VCQ8	Caldesmon 1	Cald1	13	12	6	4	1
P27659	60S ribosomal protein L3	Rpl3	7	9	1	2	1
O35737	Heterogeneous nuclear ribonucleoprotein H	Hnrnph1	4	3	1	6	0
A2ACG7	Dolichyl-diphosphooligosaccharide–protein glycosyltransferase subunit 2	Rpn2	7	3	0	6	1
Q3TVI8	Pre-B-cell leukemia transcription factor-interacting protein 1	Pbxip1	6	3	0	6	1

Table 1—*continued*

Uniprot	Description	Gene name	Σ# Peptides	Total spectrum IP1 D	Total spectrum IP1 U	Total spectrum IP2 D	Total spectrum IP2 U
F6QCI0	Protein Taf15 (fragment)	Taf15	4	3	0	6	1
O88569-3	Isoform 3 of heterogeneous nuclear ribonucleoproteins A2/B1	Hnrnpa2b1	5	4	1	6	1
O08583-2	Isoform 2 of THO complex subunit 4	Alyref	3	2	0	8	2
O08573-2	Isoform short of galectin-9	Lgals9	2	2	1	7	0
Q564E8	Ribosomal protein L4	Rpl4	8	7	3	6	2
B1ARA3	60S ribosomal protein L26 (fragment)	Rpl26	6	5	0	5	2
O35129	Prohibitin-2	Phb2	4	4	0	7	3
D3YTQ9	40S ribosomal protein S15	Rps15	3	6	1	2	0
Q6ZWX6	Eukaryotic translation initiation factor 2 subunit 1	Eif2s1	5	4	1	4	0
D3Z3R1	60S ribosomal protein L36	Gm5745	5	3	1	6	1
P17427	AP-2 complex subunit α2	Ap2a2	8	3	1	7	2
P56480	ATP synthase subunit β, mitochondrial	Atp5b	9	2	1	8	2
Q8CBM2	Aspartate-β-hydroxylase	Asph	8	4	0	6	3
Q6NVF9	Cleavage and polyadenylation specificity factor subunit 6	Cpsf6	6	4	0	6	3
Q5SQB0	Nucleophosmin	Npm1	5	6	0	2	1
Q6A0A9	Constitutive coactivator of PPARγ-like protein 1	FAM120A	5	2	0	4	0
P14576	Signal recognition particle 54-kDa protein	Srp54	4	2	0	4	0
P63087	Serine/threonine-protein phosphatase PP1γ catalytic subunit	Ppp1cc	4	4	0	2	0
P80315	T-complex protein 1 subunit δ	Cct4	4	3	0	3	0
P62960	Nuclease-sensitive element-binding protein 1	Ybx1	3	2	0	5	1
P97376	Protein FRG1	Frg1	3	2	0	5	1
Q3U4Z7	High-density lipoprotein-binding protein, isoform CRA_d	Hdlbp	7	3	0	4	1
B2RTB0	MCG17262	Pdap1	4	3	0	4	1
P60335	Poly(rC)-binding protein 1	Pcbp1	4	3	0	4	1
P47911	60S ribosomal protein L6	Rpl6	6	8	4	2	0
Q61990-2	Isoform 2 of poly(rC)-binding protein 2	Pcbp2	4	2	1	6	1
P62267	40S ribosomal protein S23	Rps23	5	4	1	6	3
D3Z148	Caveolin (fragment)	Cav1	4	2	0	3	0
P84084	ADP-ribosylation factor 5	Arf5	4	2	0	3	0
O54724	Polymerase I and transcript release factor	Ptrf	3	2	0	3	0
E9Q132	60S ribosomal protein L24	Rpl24	3	4	1	2	0
O54890	Integrin β3	Itgb3	5	3	1	3	0
O88477	Insulin-like growth factor 2 mRNA-binding protein 1	Igf2bp1	4	2	0	4	1
P61750	ADP-ribosylation factor 4	Arf4	4	2	0	4	1
Q9CR67	Transmembrane protein 33 OS	Tmem33	3	2	0	4	1
Q5XJF6	Ribosomal protein L10a	Rpl10a	7	6	3	2	0
Q3THB3	Heterogeneous nuclear ribonucleoprotein M	Hnrnpm	5	2	1	4	0
Q6P5B5	Fragile X mental retardation syndrome-related protein 2	Fxr2	5	3	1	5	2
D3Z6S1	Uncharacterized protein	Tmem214	3	2	0	2	0
P11152	Lipoprotein lipase	Lpl	3	2	0	2	0
Q9DCR2	AP-3 complex subunit σ1	Ap3s1	3	2	0	2	0
P59999	Actin-related protein 2/3 complex subunit 4	Arpc4	2	3	1	2	0
P49312	Heterogeneous nuclear ribonucleoprotein A1	Hnrnpa1	5	3	1	3	1
P61358	60S ribosomal protein L27	Rpl27	4	3	1	3	1
O54734	Dolichyl-diphosphooligosaccharide–protein glycosyltransferase 48-kDa subunit	Ddost	3	2	1	3	0
Q07235	Glia-derived nexin	Serpine2	6	2	0	4	2
Q7TNV0	Protein DEK	Dek	5	3	0	2	1
Q922B2	Aspartate–tRNA ligase, cytoplasmic	Dars	4	3	0	2	1
P62320	Small nuclear ribonucleoprotein Sm D3	Snrpd3	3	2	1	5	2
P15864	Histone H1.2	Hist1h1c	2	2	1	5	2
Q8R0W0	Epiplakin	Eppk1	3	2	1	3	1
Q6ZQ38	Cullin-associated NEDD8-dissociated protein 1	Cand1	4	2	1	2	1

ethylxanthine), supplemented with rosiglitazone (Fig. 1, *A* and *B*), and confirmed by Oil Red-O staining and *Pparg* mRNA expression (Fig. 1, *B* and *C*).

Differentiation of TAP–14-3-3ζ MEFs results in distinct changes in the interactome of 14-3-3ζ

Although we previously identified the hedgehog signaling effector, Gli3, as a downstream regulator of 14-3-3ζ-dependent adipogenesis (4), we hypothesized that 14-3-3ζ may control other parallel processes underlying adipocyte differentiation. This is due in part to the large, diverse interactomes of 14-3-3 proteins (8, 12–15). Thus, we utilized affinity proteomics to identify interacting proteins that associate with 14-3-3ζ during adipocyte differentiation (Fig. 1*A*). The interactome of 14-3-3ζ at 24 h postinduction was examined because key signaling events underlying murine adipocyte differentiation occur during the first 24–48 h (2, 4). Over 100 proteins were identified by MS as 14-3-3ζ–interacting proteins (Table 1). Of these proteins, 56 have not been previously reported to interact with any member of the 14-3-3 protein family (Table 2) (14). 14-3-3ζ itself was found equally enriched in both samples, demonstrating equal pulldown efficiency (data not shown). An enrichment of differentiation-dependent 14-3-3ζ-interacting proteins associated with RNA splicing, translation,

Table 2

Identification of novel interactors with 14-3-3 proteins

The information in this table is compared to the data of Johnson *et al.* (14). There is a total of 56 novel interactors.

Uniprot	Description	Gene name	Previously reported to interact with 14-3-3ζ
Q8VDD5	Myosin-9	Myh9	Yes
Q4FK11	Non-POU-domain-containing, octamer binding protein	Nono	No
E9QMZ5	Plectin	Plec	No
E9QPE8	Plectin	Plec	No
G5E8B8	Anastellin	Fn1	No
Q61879	Myosin-10	Myh10	Yes
P97855	Ras GTPase-activating protein-binding protein 1	G3bp1	Yes
P61979	Heterogeneous nuclear ribonucleoprotein K	Hnrnpk	Yes
Q9R002	Interferon-activable protein 202	Ifi202	No
B7FAU9	Filamin, α	Flna	No
Q61033	Lamina-associated polypeptide 2, isoforms α/ζ	Tmpo	Yes
B2RSN3	MCG1395	Tubb2b	Yes
Q91VR5	ATP-dependent RNA helicase DDX1	Ddx1	Yes
P48962	ADP/ATP translocase 1	Slc25a4	Yes
P51881	ADP/ATP translocase 2	Slc25a5	Yes
Q60865	Caprin-1	Caprin1	Yes
Q8BMK4	Cytoskeleton-associated protein 4	Ckap4	Yes
B8JJG1	Novel protein (2810405J04Rik)	Fam98a	No
Q61029	Lamina-associated polypeptide 2, isoforms β/δ/ϵ/γ	Tmpo	Yes
Q8VIJ6	Splicing factor, proline- and glutamine-rich	Sfpq	Yes
P62702	40S ribosomal protein S4, X isoform	Rps4x	Yes
Q3TQX5	DEA(D/H) (Asp-Glu-Ala-Asp/His) box polypeptide 3, X-linked	Ddx3x	No
Q4VA29	MCG140066	2700060E02Rik	No
P14148	60S ribosomal protein L7	Rpl7	Yes
Q3UMM1	Tubulin, β6	Tubb6	No
G3UXT7	RNA-binding protein FUS (fragment)	Fus	No
Q8VEM8	Phosphate carrier protein, mitochondrial	Slc25a3	Yes
E9QPE7	Myosin-11	Myh11	No
A2A547	Ribosomal protein L19	Rpl19	No
P63038	60-kDa heat shock protein, mitochondrial	Hspd1	Yes
D3Z6C3	Protein Gm10119	Gm10119	No
Q9DB20	ATP synthase subunit O, mitochondrial	Atp5o	Yes
O70475	UDP-glucose 6-dehydrogenase	Ugdh	No
A2APD4	Small nuclear ribonucleoprotein-associated protein	Snrpb	No
O70309	Integrin β5	Itgb5	No
G3UZI2	Heterogeneous nuclear ribonucleoprotein Q	Syncrip	No
D3Z6U8	Fragile X mental retardation protein 1 homolog	Fmr1	No
O35841	Apoptosis inhibitor 5	Api5	No
A4FUS1	MCG123443	Rps16	No
Q3TLH4-5	Isoform 5 of protein PRRC2C	Prrc2c	No
P14869	60S acidic ribosomal protein P0	Rplp0	Yes
Q8QZY1	Eukaryotic translation initiation factor 3 subunit L	Eif3l	No
P35922	Fragile X mental retardation protein 1 homolog	Fmr1	Yes
Q03265	ATP synthase subunit α, mitochondrial	Atp5a1	Yes
P63017	Heat shock cognate 71-kDa protein	Hspa8	Yes
P21981	Protein-glutamine γ-glutamyltransferase 2	Tgm2	Yes
Q80UM7	Mannosyl-oligosaccharide glucosidase	Mogs	Yes
P26369	Splicing factor U2AF 65-kDa subunit	U2af2	No
A2AJM8	MCG7378	Sec61b	No
P62242	40S ribosomal protein S8	Rps8	Yes
P54823	DEA(D/H) (Asp-Glu-Ala-Asp/His) box polypeptide 6	Ddx6	Yes
Q3TML6	Eukaryotic translation initiation factor 2, subunit 3, structural gene X-linked	Eif2s3x	No
P26041	Moesin	Msn	Yes
P62983	Ubiquitin-40S ribosomal protein S27a	Rps27a	Yes
P52480	Pyruvate kinase isozymes M1/M2	Pkm2	Yes
Q5SUT0	Ewing sarcoma breakpoint region 1	Ewsr1	No
E9Q7H5	Uncharacterized protein	Gm8991	No
Q8C2Q8	ATP synthase γ chain	Atp5c1	No
A2AMW0	Capping protein (actin filament) muscle Z-line, β	Capzb	No
P08121	Collagen α-1(III) chain	Col3a1	Yes
P11087-2	Isoform 2 of collagen α-1(I) chain	Col1a1	Yes
Q9Z2X1-2	Isoform 2 of heterogeneous nuclear ribonucleoprotein F	Hnrnpf	Yes
P11499	Heat shock protein HSP 90β	Hsp90ab1	Yes
P28301	Protein-lysine 6-oxidase	Lox	Yes
Q8VCQ8	Caldesmon 1	Cald1	No
P27659	60S ribosomal protein L3	Rpl3	Yes
O35737	Heterogeneous nuclear ribonucleoprotein H	Hnrnph1	Yes
A2ACG7	Dolichyl-diphosphooligosaccharide–protein glycosyltransferase subunit 2	Rpn2	No
Q3TVI8	Pre-B-cell leukemia transcription factor-interacting protein 1	Pbxip1	No
F6QCI0	Protein Taf15 (fragment)	Taf15	No
O88569-3	Isoform 3 of Heterogeneous nuclear ribonucleoproteins A2/B1	Hnrnpa2b1	Yes
O08583-2	Isoform 2 of THO complex subunit 4	Alyref	Yes
O08573-2	Isoform short of galectin-9	Lgals9	Yes
Q564E8	Ribosomal protein L4	Rpl4	No
B1ARA3	60S ribosomal protein L26 (Fragment)	Rpl26	No
O35129	Prohibitin-2	Phb2	Yes
D3YTQ9	40S ribosomal protein S15	Rps15	No
Q6ZWX6	Eukaryotic translation initiation factor 2 subunit 1	Eif2s1	Yes

Table 2—*continued*

Uniprot	Description	Gene name	Previously reported to interact with 14-3-3ζ
D3Z3R1	60S ribosomal protein L36	Gm5745	No
P17427	AP-2 complex subunit α2	Ap2a2	No
P56480	ATP synthase subunit β, mitochondrial	Atp5b	Yes
Q8CBM2	Aspartate-β-hydroxylase	Asph	No
Q6NVF9	Cleavage and polyadenylation specificity factor subunit 6	Cpsf6	Yes
Q5SQB0	Nucleophosmin	Npm1	No
Q6A0A9	Constitutive coactivator of PPARγ-like protein 1	FAM120A	Yes
P14576	Signal recognition particle 54-kDa protein	Srp54	No
P63087	Serine/threonine-protein phosphatase PP1γ catalytic subunit	Ppp1cc	Yes
P80315	T-complex protein 1 subunit δ	Cct4	Yes
P62960	Nuclease-sensitive element-binding protein 1	Ybx1	Yes
P97376	Protein FRG1	Frg1	No
Q3U4Z7	High-density lipoprotein-binding protein, isoform CRA_d	Hdlbp	No
B2RTB0	MCG17262	Pdap1	No
P60335	Poly(rC)-binding protein 1	Pcbp1	Yes
P47911	60S ribosomal protein L6	Rpl6	Yes
Q61990-2	Isoform 2 of Poly(rC)-binding protein 2	Pcbp2	Yes
P62267	40S ribosomal protein S23	Rps23	Yes
D3Z148	Caveolin (Fragment)	Cav1	No
P84084	ADP-ribosylation factor 5	Arf5	Yes
O54724	Polymerase I and transcript release factor	Ptrf	Yes
E9Q132	60S ribosomal protein L24	Rpl24	No
O54890	Integrin β-3	Itgb3	No
O88477	Insulin-like growth factor 2 mRNA-binding protein 1	Igf2bp1	Yes
P61750	ADP-ribosylation factor 4	Arf4	Yes
Q9CR67	Transmembrane protein 33 OS	Tmem33	Yes
Q5XJF6	Ribosomal protein L10a	Rpl10a	No
Q3THB3	Heterogeneous nuclear ribonucleoprotein M	Hnrnpm	No
Q6P5B5	Fragile X mental retardation syndrome-related protein 2	Fxr2	No
D3Z6S1	Uncharacterized protein	Tmem214	No
P11152	Lipoprotein lipase	Lpl	Yes
Q9DCR2	AP-3 complex subunit σ1	Ap3s1	No
P59999	Actin-related protein 2/3 complex subunit 4	Arpc4	Yes
P49312	Heterogeneous nuclear ribonucleoprotein A1	Hnrnpa1	Yes
P61358	60S ribosomal protein L27	Rpl27	Yes
O54734	Dolichyl-diphosphooligosaccharide–protein glycosyltransferase 48-kDa subunit	Ddost	Yes
Q07235	Glia-derived nexin	Serpine2	No
Q7TNV0	Protein DEK	Dek	Yes
Q922B2	Aspartate–tRNA ligase, cytoplasmic	Dars	No
P62320	Small nuclear ribonucleoprotein Sm D3	Snrpd3	Yes
P15864	Histone H1.2	Hist1h1c	Yes
Q8R0W0	Epiplakin	Eppk1	No
Q6ZQ38	Cullin-associated NEDD8-dissociated protein 1	Cand1	Yes

protein transport, and nucleic acid transport was detected using gene ontology to define their biological processes (17) (Table 3). Thus, these proteomic data demonstrate the dynamic nature of the 14-3-3ζ interactome and suggest that 14-3-3ζ may regulate multiple processes, such as RNA processing, during adipocyte differentiation.

Identification of known regulators of adipocyte differentiation in the 14-3-3ζ interactome

We were able to detect proteins with known and purported roles in adipogenesis, such as Ptrf/Cavin1, Phb2, Fragile-X mental retardation protein-1 (Fmr1), and Rpn2, through our proteomic analysis of the 14-3-3ζ interactome (Table 1 and Fig. 1*D*) (18–23). These proteins do not have any purported roles in RNA splicing. Using siRNA-mediated knockdown approaches, we examined their roles in adipocyte differentiation, as assessed by Oil Red-O incorporation and *Pparg* mRNA and Pparγ protein measurements (Fig. 2 and Fig. S1*A*). Of the factors examined, only knockdown of Ptrf/Cavin1 attenuated 3T3-L1 adipogenesis (Fig. 2 and Fig. S1*A*). When taken together, these findings highlight the ability of identifying known regulators of adipogenesis within the 14-3-3ζ interactome and suggest the possibility that novel adipogenic factors can also be identified through this approach.

Requirement of RNA processing during adipogenesis

Because enrichments in RNA splicing proteins were detected in the 14-3-3ζ interactome during differentiation (Table 1), it suggested that 14-3-3ζ could influence pre-mRNA processing during adipogenesis. Splicing is mediated by the spliceosome complex, which removes intronic regions from pre-mRNA (constitutive) or facilitates alternative splicing of mRNA at regulatory regions enriched with splicing factors (24). Initially, the spliceosome inhibitor, madrasin, was used to examine the requirement of the spliceosome during adipocyte differentiation (25), and inhibition of the spliceosome blocked adipogenesis (Fig. 3, *A* and *B*). Pre-mRNA of the canonical adipogenic gene, *Pparg*, undergoes alternative splicing to yield *Pparg1* and *Pparg2* mRNAs, which are further translated into Pparγ isoforms, Pparγ1 and Pparγ2 (26–29). To examine whether the spliceosome is involved in processing of *Pparg* mRNA, we utilized quantitative PCR to measure mRNA levels of *Pparg1*, *Pparg2*, and a novel *Pparg1* variant, *Pparg1sv* (29). Spliceosome inhibition significantly reduced the expression of the *Pparg2* and *Pparg1sv* mRNA (Fig. 3*B*). Thus, the activity of the spliceosome is required for adipocyte differentiation.

Within the adipocyte differentiation-associated 14-3-3ζ interactome, U2AF, a component of the spliceosome, was

Table 3
Gene ontology classification of proteomic hits by biological process
FDR, false discovery rate.

		p value	Benjamini	FDR
Annotation cluster 1 (enrichment score: 10.542304553852539)				
GO:0006397	mRNA processing	2.80E-12	1.18E-09	4.33E-09
GO:0008380	RNA splicing	8.22E-12	2.31E-09	1.27E-08
GO:0016071	mRNA metabolic process	2.70E-11	5.71E-09	4.18E-08
GO:0006396	RNA processing	1.09E-09	1.84E-07	1.68E-06
Annotation cluster 2 (enrichment score: 2.9768010746589035)				
GO:0065003	Macromolecular complex assembly	1.23E-04	0.01719154	0.19018503
GO:0006461	Protein complex assembly	1.87E-04	0.01956598	0.28880909
GO:0070271	Protein complex biogenesis	1.87E-04	0.01956598	0.28880909
GO:0043933	Macromolecular complex subunit organization	2.40E-04	0.02229116	0.37052613
GO:0034621	Cellular macromolecular complex subunit organization	0.001634086	0.10877737	2.49672826
GO:0034622	Cellular macromolecular complex assembly	0.004135111	0.20818502	6.20540124
GO:0043623	Cellular protein complex assembly	0.00690653	0.26524962	10.1607298
GO:0051258	Protein polymerization	0.031762743	0.57358582	39.2881889
Annotation cluster 3 (enrichment score: 2.7758570598049186)				
GO:0015931	Nucleobase, nucleoside, nucleotide, and nucleic acid transport	1.65E-04	0.01976438	0.25533903
GO:0051236	Establishment of RNA localization	0.001160158	0.09343294	1.77868077
GO:0050658	RNA transport	0.001160158	0.09343294	1.77868077
GO:0050657	Nucleic acid transport	0.001160158	0.09343294	1.77868077
GO:0006403	RNA localization	0.001227278	0.09002225	1.88067318
Annotation cluster 4 (enrichment score: 1.3081305561358054)				
GO:0015986	ATP synthesis-coupled proton transport	0.002165467	0.13143078	3.29598278
GO:0015985	Energy-coupled proton transport, down electrochemical gradient	0.002165467	0.13143078	3.29598278
GO:0034220	Ion transmembrane transport	0.00311983	0.17188096	4.71608221
GO:0015992	Proton transport	0.005711473	0.26103289	8.47469156
GO:0006818	Hydrogen transport	0.006023853	0.24696352	8.91824507
GO:0006119	Oxidative phosphorylation	0.007021577	0.25748192	10.3215008
GO:0006754	ATP biosynthetic process	0.019701699	0.53433002	26.4817286
GO:0046034	ATP metabolic process	0.025117659	0.59165663	32.5166079
GO:0009201	Ribonucleoside triphosphate biosynthetic process	0.027334987	0.59373718	34.8509636
GO:0009206	Purine ribonucleoside triphosphate biosynthetic process	0.027334987	0.59373718	34.8509636
GO:0009145	Purine nucleoside triphosphate biosynthetic process	0.028096637	0.59012787	35.6352295
GO:0009142	Nucleoside triphosphate biosynthetic process	0.02886954	0.5741125	36.4220479
GO:0009205	Purine ribonucleoside triphosphate metabolic process	0.033742375	0.58476996	41.1791708
GO:0009199	Ribonucleoside triphosphate metabolic process	0.034593574	0.58312761	41.9751939
GO:0006091	Generation of precursor metabolites and energy	0.03610049	0.58839461	43.3597731
GO:0009144	Purine nucleoside triphosphate metabolic process	0.038109124	0.58825354	45.1573304
GO:0009152	Purine ribonucleotide biosynthetic process	0.039015563	0.58726975	45.9509181
GO:0055085	Transmembrane transport	0.042081945	0.60604395	48.5566327
GO:0009260	Ribonucleotide biosynthetic process	0.042750615	0.59362044	49.1090183
GO:0009141	Nucleoside triphosphate metabolic process	0.046658895	0.60897427	52.228246
Annotation cluster 5 (enrichment score: 1.1516193992206216)				
GO:0001568	Blood vessel development	0.028163983	0.57774561	35.7041482
GO:0001944	Vasculature development	0.030823763	0.58598984	38.3715132

detected (Table 1) (24). This suggests that 14-3-3ζ may influence the activity of the spliceosome during adipogenesis through its interactions. Focusing on *Pparg*, we found that siRNA-mediated depletion of 14-3-3ζ significantly blocked the increase in total *Pparg* mRNA levels and attenuated the production of *Pparg1*, *Pparg2*, and *Pparg1sv* splice variants (Fig. 3*C*). Furthermore, significantly decreased abundance of Pparγ1 and Pparγ2 protein was detected in 14-3-3ζ-depleted cells (Fig. 3, *D* and *E*). When taken together, these findings demonstrate the importance of the spliceosome and suggest indirect actions of 14-3-3ζ in the splicing of key adipogenic mRNAs.

Regulation of mRNA processing by 14-3-3ζ during adipocyte differentiation

To gain a better understanding of the global effects of 14-3-3ζ depletion on mRNA splicing, we utilized our previous transcriptomic analysis from control and 14-3-3ζ-depleted 3T3-L1 cells undergoing differentiation (4). Differential exon usage (DEXSeq) was used as a surrogate measure of alternative splicing of mRNA (Fig. 4*A*) (30). Any changes in splice variant levels were not due to global effects of 14-3-3ζ depletion on RNA transcription because no gross differences in the incorporation of a uracil analog were detected (Fig. 4*B*). At 24 and 48 h post-differentiation, 163 and 172 unique genes, respectively, were found to undergo differential exon usage (Fig. 4*C*). Gene ontology analysis revealed that at each time point, distinct groups of genes were alternatively spliced (Table 4). The use of this approach to detect genes with DEXSeq was validated by the ability to detect alternative exon usage in *Pparg* after 48 h of differentiation (Fig. S2) (28). The effect of 14-3-3ζ depletion was assessed at each time point, and 78, 37, and 36 genes were affected following 14-3-3ζ knockdown at 0, 24, and 48 h, respectively, after the induction of differentiation (Fig. 4*D*). However, only in undifferentiated 3T3-L1 cells could enrichments in genes associated with macromolecular complex

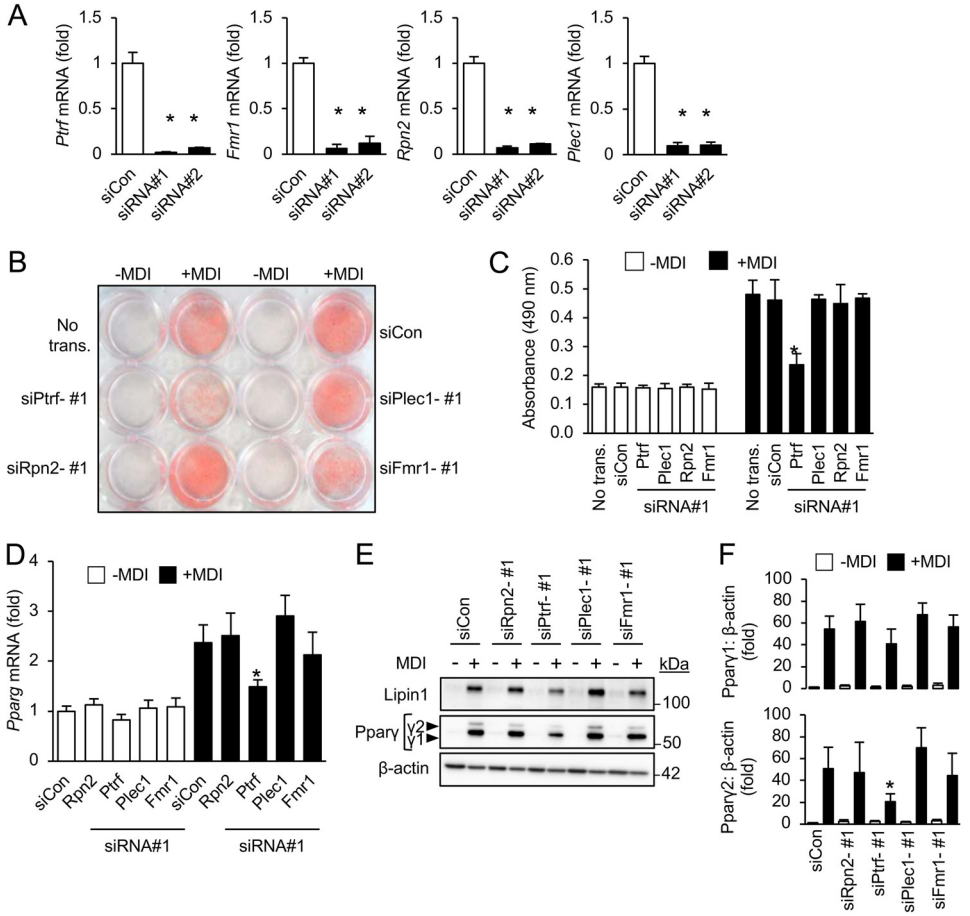

Figure 2. Known regulators of adipogenesis can be found within the 14-3-3ζ interactome. *A*, 3T3-L1 cells were transfected with a control siRNA (siCon) or two independent siRNAs (siRNAs 1 and 2) against target mRNA, and knockdown efficiency was measured by quantitative PCR ($n = 4$ per group; *, $p < 0.05$ when compared with siCon-transfected cells; *bar graphs* represent means ± S.D.). *B* and *C*, transient knockdown by siRNA of previously identified regulators of adipogenesis or those associated with the development of obesity was used to examine their contributions to adipocyte differentiation (+MDI), as assessed by visualization of Oil Red-O incorporation (*B*), absorbance (490 nm, *C*) (*, $p < 0.05$ when compared with siCon + MDI; *bar graphs* represent means ± S.D.). *D–F*, measurement of total *Pparg* mRNA levels (*D*) or Pparγ protein abundance (*E* and *F*) in siCon or siRNA-transfected 3T3-L1 cells induced to differentiate (+MDI) for 48 h ($n = 4$ per group; *, $p < 0.05$ when compared with siCon-transfected differentiated cells; *bar graphs* represent means ± S.D.).

assembly (GO:0065003, $p = 3.44 \times 10^{-3}$), macromolecular complex subunit organization (GO:0043933, $p = 7.56 \times 10^{-4}$), and regulation of biological quality (GO:0065008, $p = 9.51 \times 10^{-3}$) be detected by gene ontology analysis. Collectively, these data demonstrate that adipogenesis promotes the alternative splicing of genes, and this process can be influenced by 14-3-3ζ.

Requirement of RNA-splicing factors in adipocyte differentiation

14-3-3ζ is not a *bona fide* splicing factor, and it is likely that specific RNA-splicing factors within its interactome are responsible for the observed effects on differential exon usage (Fig. 4*D*). Transient transfection of siRNA in 3T3-L1 pre-adipocytes against eight splicing factors identified in our proteomic analysis of the 14-3-3ζ interactome (Table 1) was performed to examine their roles in 3T3-L1 adipogenesis (Fig. 5 and Fig. S1*B*). They were chosen by the number of connections exhibited within each cluster of proteins (Fig. 1*D*) (17). Transcript levels of the chosen splicing factors, as determined by RNA-Seq, were generally unaffected by knockdown of 14-3-3ζ; however, some splicing factors were influenced by differentiation (Fig. S3) (GEO accession code GSE60745). Knockdown of Ddx6, Sfpq, Hnrpf, or Hnrpk was sufficient to impair 3T3-L1 differentiation, as assessed by Oil Red-O incorporation and total *Pparg* mRNA expression (Fig. 5 and Fig. S1*B*). Closely related proteins with similar roles, such as Ddx1, Nono, Hnrpm, and Syncrip (Hnrpq) were not required for 3T3-L1 adipogenesis (Fig. 5 and Fig. S1*B*).

To further explore the role of splicing factors within the 14-3-3ζ interactome, we examined the impact of their depletion on *Pparg* mRNA splice variant formation and Pparγ protein abundance. In undifferentiated cells, knockdown of *Hnrnpf* and *Ddx6* had effects on the levels of *Pparg1* or *Pparg2* mRNA (Fig. 6*A*). However, in differentiating 3T3-L1 cells, only knockdown of *Hnrnpf* and *Sfpq* were found to significantly reduce *Pparg2* or *Pparg1sv* mRNA levels (Fig. 6*A*). Pparγ1 and Pparγ2 protein levels differed from what was observed with the pattern of *Pparg* mRNA variants. Ddx6-depleted cells exhibited significantly decreased Pparγ1 abundance, whereas all siRNA-transfected cells significantly reduced Pparγ2 (Fig. 6, *B* and *C*). Another adipogenic gene that undergoes alternative splicing is *Lpin1.* This results in the generation of splice variants, Lipin-1α and Lipin-1β, which have differen-

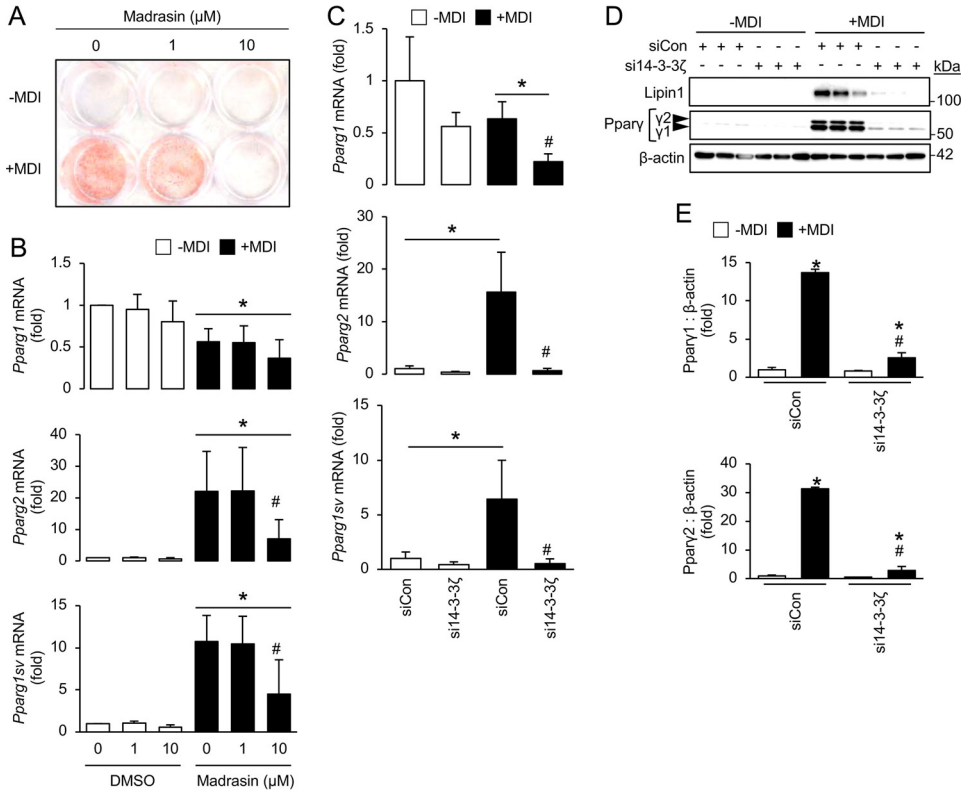

Figure 3. Inhibition of the spliceosome or depletion of 14-3-3ζ prevents the alternative splicing of *Pparg* mRNA. *A*, 3T3-L1 cells were incubated with 1 or 10 μM madrasin in the presence of the adipogenic differentiation mixture (MDI), followed by differentiation for 7 days. Adipogenesis was assessed by Oil Red-O incorporation (representative of $n = 5$ independent experiments). *B*, RNA was isolated from madrasin-treated cells induced to differentiate for 48 h, and quantitative PCR was used to measure *Pparg* splice variants ($n = 5$ per group; *, $p < 0.05$ when compared with undifferentiated cells; #, $p < 0.05$ when compared with 0 μM madrasin, differentiated cells; *bar graphs* represent means ± S.D.). *C*, 3T3-L1 cells were transfected with siRNA against 14-3-3ζ or siCon and differentiated for 48 h, followed by isolation of total RNA to measure *Pparg* splice variants by quantitative PCR ($n = 4$ per group; *, $p < 0.05$ when compared with undifferentiated siCon-transfected cells; #, $p < 0.05$ when compared with differentiated, siCon-transfected cells; *bar graphs* represent means ± S.D.). *D* and *E*, 3T3-L1 cells were transfected with siRNA against 14-3-3ζ or siCon and differentiated for up to 7 days, followed by isolation of protein to measure Pparγ isoforms by immunoblotting (*D*). Protein abundance for each Pparγ isoform was measured by densitometry (*E*) ($n = 4$ per group; *, $p < 0.05$ when compared with undifferentiated siCon-transfected cells; #, $p < 0.05$ when compared with differentiated, siCon-transfected cells; *bar graphs* represent means ± S.D.).

tial roles on adipogenesis (32). To examine the effect of depletion of 14-3-3ζ, Hnrpf, Ddx6, Hnrpk, and Sfpq on *Lpin1* splicing, 3T3-L1 cells were transiently transfected with siRNA, followed by the induction of differentiation. Gene silencing of all target genes decreased the generation of the *Lpin-1α* variant during differentiation (Fig. S4). Of note, the commercially available antibody used to detect mature Lipin-1 could not differentiate between either splice variant, but knockdown of 14-3-3ζ, Hnrpf, Ddx6, Hnrpk, and Sfpq reduced total Lipin-1 abundance (Fig. 3*D* and 6*B*). Collectively, these findings demonstrate that novel regulators of adipogenesis can be identified within the interactome of 14-3-3ζ and highlight novel roles of splicing factors in the development of a mature adipocyte.

Discussion

In the present study, affinity proteomics was used to determine how adipogenesis influences the interactome of 14-3-3ζ. Surprisingly, the interactome was dynamic, because differentiation altered the landscape of proteins that interact with 14-3-3ζ. This approach permitted the identification of processes that may be regulated by 14-3-3ζ during adipocyte differentiation and led to the discovery of novel adipogenic factors within the 14-3-3ζ interactome that are required for adipocyte differentiation. Namely, an enrichment of proteins associated with RNA processing and splicing was detected, and the novel contributions of RNA-splicing factors, such as Hnrpf, Ddx6, and Sfpq, in adipogenesis were identified. Future in-depth analysis of all 14-3-3ζ–interacting partners may reveal novel factors and pathways that facilitate adipocyte differentiation and may aid in the development of approaches to control adipogenesis as a means to treat obesity.

We previously identified an essential function of the hedgehog signaling effector Gli3 in 14-3-3ζ-regulated adipocyte differentiation (4). However, because of the large, diverse interactome of 14-3-3 proteins (10, 14), we hypothesized that it is unlikely that one protein would be solely responsible for 14-3-3ζ–mediated adipogenesis. It is known that the interactomes of 14-3-3 proteins are dynamic and change in response to various stimuli (8, 10–15). The functional significance of such changes in the interactome is not clear, but it suggests that 14-3-3 proteins may regulate biological processes critical for adipocyte development through their interactions. Using a gene onotology-based approach, we found that the 14-3-3ζ interactome is enriched with proteins involved in RNA binding and splicing during differentiation and identified its contribution to the alternative splicing of mRNAs. Because over 100 proteins were found to be unique to the 14-3-3ζ interactome during adipocyte

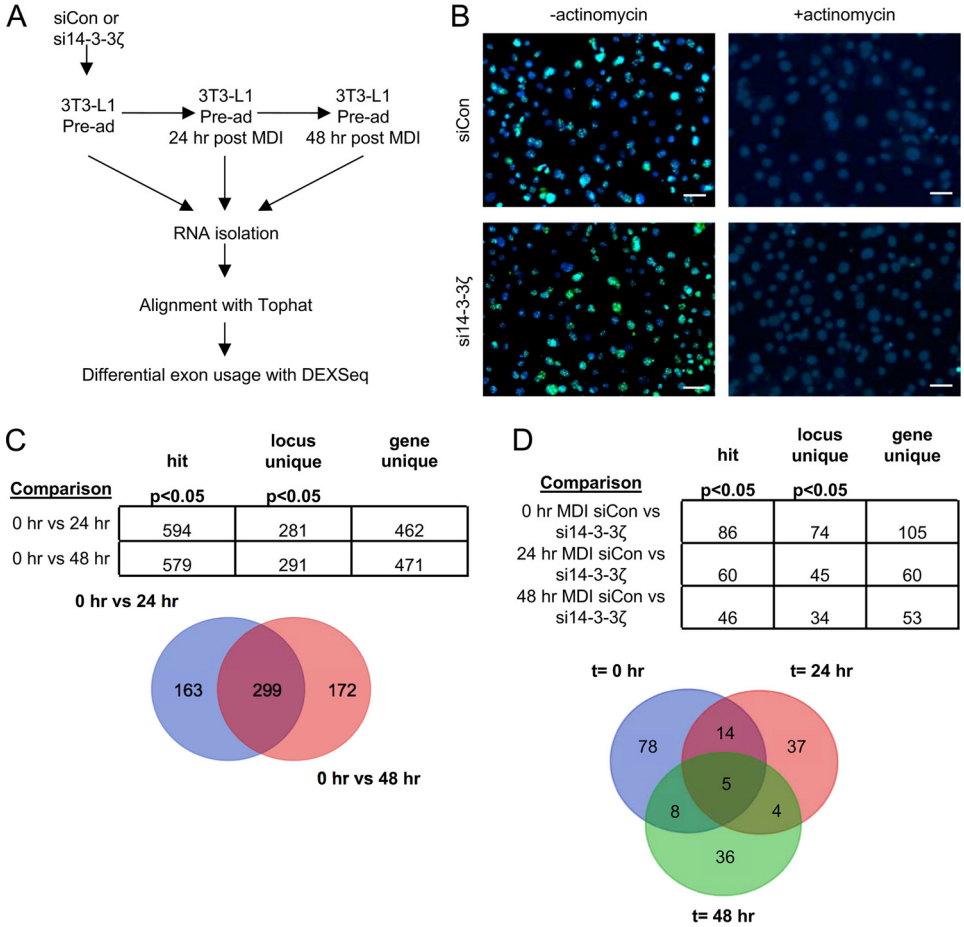

Figure 4. Induction of differentiation or depletion of 14-3-3ζ in 3T3-L1 cells promotes alternative splicing of mRNA. *A*, differential exon usage of genes involved in adipogenesis was compared in control or 14-3-3ζ-depleted 3T3-L1 cells undergoing adipocyte differentiation. Transcriptomic data were aligned via TopHat and subsequently subjected to DEXSeq analysis to measure differential exon usage. *B*, to rule out an effect of 14-3-3ζ depletion on global RNA transcription, siCon, or 14-3-3ζ depleted cells (si14-3-3ζ) were incubated with 5-ethynyl uridine, followed by Click-iT chemistry to detect newly synthesized RNA (*scale bars*, 10 μm; representative of $n = 4$ experiments). *C* and *D*, comparison of genes exhibiting differential exon usage in control cells 0, 24, and 48 h after differentiation (*C*) or control or 14-3-3ζ depleted cells at each time point (*D*). The overlapping regions of each Venn diagram denote genes that are common to each condition or treatment.

differentiation, it suggests that 14-3-3ζ may also regulate other cellular processes required for adipocyte development. For example, we detected an interaction of 14-3-3ζ with the mitochondrial regulator, Phb2 (Prohibitin-2) (Table 1), which others have shown to be essential for the expansion of mitochondria mass and mitochondrial function during adipogenesis (18, 19). Further in-depth studies are required to assess whether 14-3-3ζ has regulatory roles in mitochondrial dynamics, but when taken together, it demonstrates the possibility of examining the individual contributions of interacting partners to elucidate key biological processes required for adipocyte differentiation.

The spliceosome is responsible for constitutive and alternative splicing of mRNA, whereby intronic regions of mRNA are removed or sections of mRNA enriched with splicing factors at regulatory elements are removed, respectively (24). Various splicing factors have been found to be important for adipogenesis (33, 34), but no studies have directly tested the role of the spliceosome in this process. To this end, we found that inhibition of the spliceosome with madrasin was sufficient to block 3T3-L1 adipogenesis and prevent the generation of various *Pparg* splice variants. In our analysis of the 14-3-3ζ interactome, we detected the interaction of 14-3-3ζ with U2AF, a component of the spliceosome. 14-3-3ζ-associated interactions can modulate the activity of interacting partners (4, 35), suggesting that 14-3-3ζ could influence the activity of the spliceosome and interfere with processes associated with constitutive or alternative splicing. Although the approaches used in the present study were unable to measure effects on constitutive splicing, we were able to detect changes in alternative splicing at the level of *Pparg* and from whole transcriptome data (4). The exact mechanisms by which 14-3-3ζ is able to influence alternative splicing is not known, and 14-3-3ζ is likely dependent on the specific splicing factors that it interacts with during differentiation.

Through the use of a functional siRNA screen, we identified novel adipogenic roles of various RNA-splicing factors involved in alternative splicing. These include Hnrpf, Hnrpk, Ddx6, and Sfpq. Sfpq belongs to the DHBS (*Drosophila* behavior/human splicing) protein family and is required for transcriptional regulation (36, 37). Although a recent study by Wang *et al.* (38) found no effect of forced overexpression of Nono and Sfpq on adipogenesis, we report that Sfpq depletion impairs adipocyte differentiation. DHBS proteins may exhibit redundant, com-

Table 4
Analysis of common and unique genes during the first 48 h of 3T3-L1 adipogenesis

Comparison	GO biological process complete	*Mus musculus*: REFLIST (22221)	upload_1				
			230	Expected	Over/ under	Fold enrichment	*p* value
Common to all time points	Xenobiotic glucuronidation (GO:0052697)	9	9	0.09	+	96.61	9.70E-12
	Flavonoid glucuronidation (GO:0052696)	9	9	0.09	+	96.61	9.70E-12
	Flavonoid metabolic process (GO:0009812)	11	9	0.11	+	79.05	5.80E-11
	Cellular glucuronidation (GO:0052695)	12	9	0.12	+	72.46	1.26E-10
	Uronic acid metabolic process (GO:0006063)	13	9	0.13	+	66.89	2.56E-10
	Glucuronate metabolic process (GO:0019585)	13	9	0.13	+	66.89	2.56E-10
	Cellular response to xenobiotic stimulus (GO:0071466)	50	10	0.52	+	19.32	1.68E-06
	Xenobiotic metabolic process (GO:0006805)	46	9	0.48	+	18.9	1.66E-05
	Response to xenobiotic stimulus (GO:0009410)	56	10	0.58	+	17.25	4.95E-06
	Monosaccharide metabolic process (GO:0005996)	152	12	1.57	+	7.63	7.67E-04
	Single-organism carbohydrate metabolic process (GO:0044723)	301	15	3.12	+	4.81	6.68E-03
	Cell adhesion (GO:0007155)	754	35	7.8	+	4.48	1.34E-09
	Biological adhesion (GO:0022610)	764	35	7.91	+	4.43	1.95E-09
	Carbohydrate metabolic process (GO:0005975)	385	17	3.98	+	4.27	6.36E-03
	Cell–cell signaling (GO:0007267)	792	34	8.2	+	4.15	2.62E-08
	Nervous system development (GO:0007399)	2086	50	21.59	+	2.32	1.40E-04
	Multicellular organism development (GO:0007275)	4498	76	46.56	+	1.63	3.16E-02
	Single-organism developmental process (GO:0044767)	5073	85	52.51	+	1.62	8.08E-03
	Developmental process (GO:0032502)	5112	85	52.91	+	1.61	1.12E-02
	Primary metabolic process (GO:0044238)	7337	113	75.94	+	1.49	2.66E-03
	Cellular metabolic process (GO:0044237)	7109	109	73.58	+	1.48	7.04E-03
	Organic substance metabolic process (GO:0071704)	7692	117	79.62	+	1.47	2.59E-03
	Metabolic process (GO:0008152)	8159	122	84.45	+	1.44	2.85E-03
	Single-organism cellular process (GO:0044763)	8646	129	89.49	+	1.44	8.63E-04
	Cellular process (GO:0009987)	13696	182	141.76	+	1.28	8.17E-05
	G-protein–coupled receptor signaling pathway (GO:0007186)	1803	3	18.66	-	< 0.2	4.79E-02
Unique to 24 h	Negative regulation of response to cytokine stimulus (GO:0060761)	43	5	0.24	+	21.01	4.10E-02
	DNA repair (GO:0006281)	400	12	2.21	+	5.42	2.22E-02
	Cellular response to DNA damage stimulus (GO:0006974)	618	15	3.42	+	4.38	1.60E-02
	Cellular macromolecular complex assembly (GO:0034622)	624	15	3.45	+	4.34	1.80E-02
	Cellular macromolecule metabolic process (GO:0044260)	5396	60	29.87	+	2.01	2.97E-05
	Macromolecule metabolic process (GO:0043170)	6113	66	33.84	+	1.95	7.53E-06
	Cellular nitrogen compound metabolic process (GO:0034641)	4081	44	22.59	+	1.95	3.18E-02
	Primary metabolic process (GO:0044238)	7337	78	40.61	+	1.92	4.49E-08
	Organic substance metabolic process (GO:0071704)	7692	80	42.58	+	1.88	5.30E-08
	Nitrogen compound metabolic process (GO:0006807)	6786	69	37.56	+	1.84	3.16E-05
	Cellular metabolic process (GO:0044237)	7109	72	39.35	+	1.83	1.07E-05
	Metabolic process (GO:0008152)	8159	80	45.16	+	1.77	1.51E-06
	Cellular process (GO:0009987)	13696	101	75.81	+	1.33	6.09E-03
Unique to 48 h	Positive regulation of molecular function (GO:0044093)	1317	23	7.88	+	2.92	3.07E-02

pensatory functions (39), but given that only Sfpq depletion impaired 3T3-L1 adipogenesis, it suggests specific protein–protein or protein–nucleic acid interactions occur may with each DHBS member in the context of differentiation (37). We were also able to detect novel adipogenic roles of Hnrpf and Hnrpk, members of the heterogeneous nuclear ribonucleoproteins (Hnrps), which facilitate mRNA splicing (40, 41). Alternative splicing of mRNA is critical for maintaining genetic diversity and cell identity, in addition to the expression of key factors required for differentiation (42, 43). Specific to adipogenesis, differential promoter usage and alternative splicing are required for the expression of the canonical adipogenic transcription factor Pparγ (26–28, 43). Other regulatory factors are also formed from alternative splicing, including nCOR1 and Lipin1 (33, 43, 44). In the present study, we identified distinct roles of each splicing factor in generating *Pparg* mRNA splice variants. Not all tested splicing factors had significant effects on *Pparg* mRNA or total Pparγ protein levels, despite being required for differentiation. It is likely that they control the splicing of other genes, such as *Lpin-1*, that are required for adipogenesis. Thus, future studies aimed at elucidating the generation of splice variants by each splicing factor would greatly increase the current knowledge of key factors required for adipocyte development.

Protein abundance of 14-3-3ζ and other isoforms is increased in visceral adipose tissue from obese individuals (45, 46), and we have previously reported that systemic overexpression of 14-3-3ζ in mice is sufficient to potentiate weight gain and fat mass in mice fed a high-fat diet (4). With respect to the pancreatic β-cell, single-cell transcriptomic analysis revealed higher mRNA expression of *YWHAZ* in β-cells from subjects with type 2 diabetes (47), and we have found that systemic overexpression of 14-3-3ζ was sufficient to reduce β-cell secretory function in mice (9). The exact mechanisms of how changes in 14-3-3ζ function affect the development of obesity or β-cell dysfunction are not known, but in-depth examination of the interactome, in addition to how 14-3-3ζ may influence the generation of splice variants, in the context of both conditions may yield novel biological insight as to how 14-3-3ζ influences the development of either disease. This approach has already been useful in understanding how changes in 14-3-3ϵ or 14-3-3σ expression promote the development of various forms of cancer and the identification of novel therapeutic targets (48, 49).

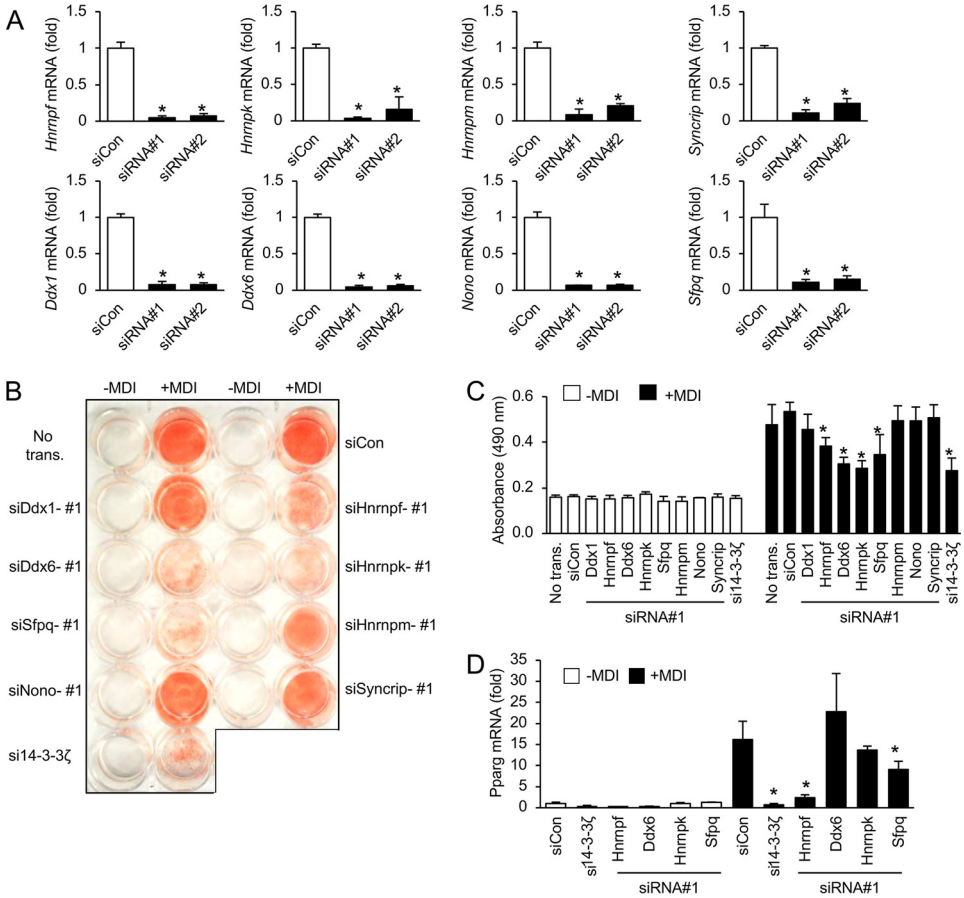

Figure 5. RNA splicing proteins are required for 3T3-L1 adipogenesis. *A*, 3T3-L1 cells were transfected with a siCon or two independent siRNAs (siRNAs 1 and 2) against target mRNA, and knockdown efficiency was measured by quantitative PCR ($n = 4$ per group; *, $p < 0.05$; *bar graphs* represent means ± S.D.). *B–D*, transient knockdown by siRNA was used to examine the contributions of RNA-splicing factors to adipocyte differentiation (+MDI), as assessed by visualization of Oil Red-O incorporation (*B*), absorbance associated with Oil Red-O (490 nm, *C*), or *Pparg* mRNA expression (*D*) ($n = 4$ per group; *, $p < 0.05$ when compared with differentiated, siCon-transfected cells; *bar graphs* represent means ± S.D.).

In conclusion, this study provides compelling evidence demonstrating the usefulness of elucidating the interactome of 14-3-3ζ as a means to identify novel factors required for adipogenesis. Additionally, a systematic investigation of interacting partners may also provide insight as to which physiological processes are essential for 14-3-3ζ–mediated adipocyte differentiation. Lastly, deciphering how various disease states influence the interactome of 14-3-3 proteins may also aid in the discovery of novel therapeutic targets for the treatment of chronic diseases, such as obesity and type 2 diabetes.

Experimental procedures

Generation of TAP–14-3-3ζ MEFs and cell culture

All animal procedures were approved and conducted in accordance with guidelines set by the University of British Columbia Animal Care Council. Embryos at embryonic day 13.5 were harvested from pregnant transgenic mice overexpressing a TAP-epitope–tagged 14-3-3ζ molecule (4), and MEFs were generated according to established protocols. 3T3-L1 cells (between passages 11 and 17) and MEFs were maintained in 25 mM glucose DMEM, supplemented with 10% newborn calf serum or fetal bovine serum, respectively, and 1% penicillin/streptomycin (ThermoFisher Scientific, Waltham, MA). Differentiation of MEFs and 3T3-L1 cells was induced with DMEM, supplemented with 10% fetal bovine serum, 172 nM insulin, 500 μM isobutylmethylxanthine, and 500 nM dexamethasone (MDI). Differentiation medium for MEFs was further supplemented with rosiglitazone (Sigma–Aldrich). Following incubation with differentiation medium for 2 days, the medium was replaced every 2 days with 25 mM glucose DMEM, supplemented with 10% fetal bovine serum and 172 nM insulin. Differentiation was assessed by Oil Red-O incorporation (Sigma–Aldrich), as previously described (4). To inhibit pre-mRNA processing, 3T3-L1 cells were incubated with the spliceosome inhibitor, madrasin (Sigma–Aldrich), during incubation with differentiation medium (25).

Mass spectrometry

Equal amounts of cell lysates from undifferentiated and differentiated TAP–14-3-3ζ MEFs were subjected to an overnight incubation with IgG coupled to protein G beads (ThermoFisher Scientific) in radioimmune precipitation assay buffer. Bound proteins from each pulldown were eluted with 1× SDS sample buffer without reducing agents and separated by SDS-PAGE prior to in-gel digestion (50). For each sample, peptides from three fractions (<50 kDa, >50 kDa, and IgG bands) were then purified on C-18 stage tips (51) and analyzed using a LTQ-Orbitrap Velos (ThermoFisher Scientific) as previ-

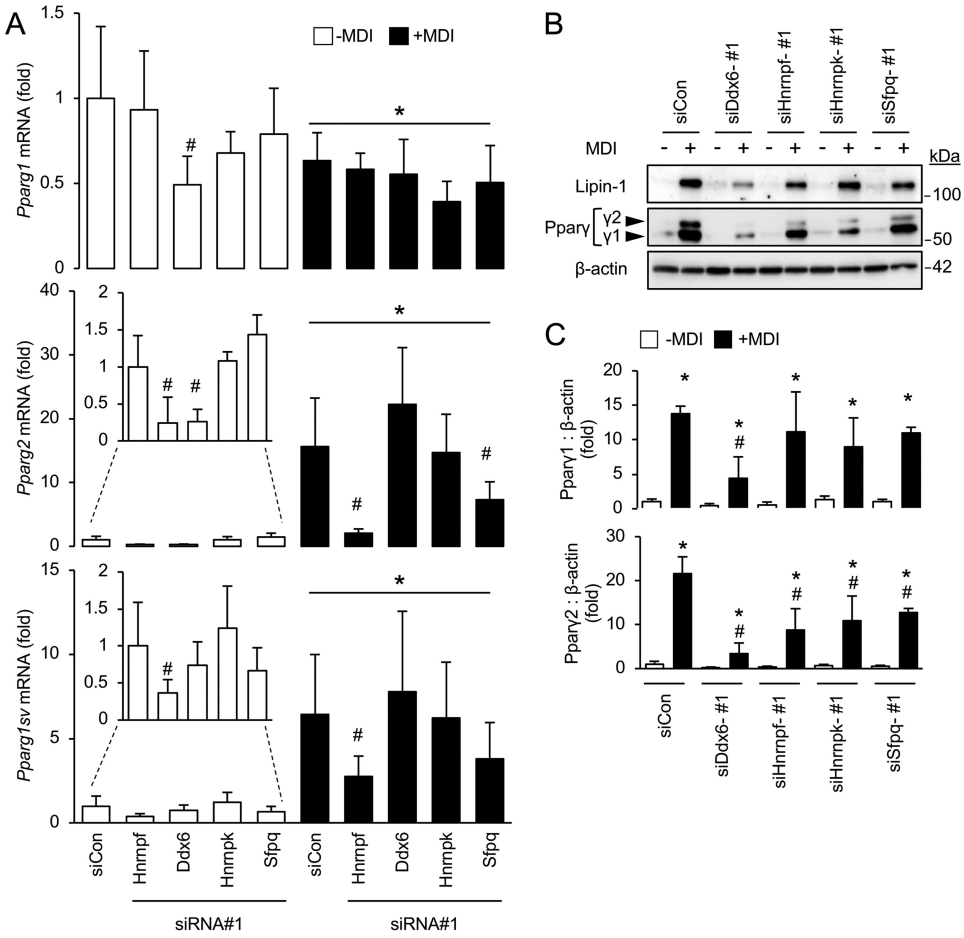

Figure 6. siRNA-mediated knockdown of identified splicing factors in the 14-3-3ζ interactome alters the splicing of *Pparg* mRNA. *A*, 3T3-L1 pre-adipocytes were transfected with siCon or target-specific siRNAs, followed by differentiation (+MDI) for 48 h. Total RNA was isolated, and quantitative PCR was used to measure *Pparg* mRNA splice variants ($n = 4$ per group; *, $p < 0.05$ when compared with undifferentiated siCon-transfected cells; #, $p < 0.05$ when compared with differentiated, siCon-transfected cells; *bar graphs* represent means ± S.D.). *B* and *C*, 3T3-L1 pre-adipocytes were transfected with siCon or target-specific siRNAs, followed by differentiation (+MDI) for up to 7 days. Following isolation of total cell lysates, immunoblotting was performed to measure Pparγ1 or 2 and Lipin-1 protein abundance (*B*). Densitometric analysis was utilized to assess the impact of target knockdown on Pparγ1 or 2 abundance (*C*) ($n = 4$ per group; *, $p < 0.05$ when compared with undifferentiated siRNA-transfected cells; #, $p < 0.05$ when compared with differentiated siCon-transfected cells; *bar graphs* represent means ± S.D.).

ously described (52). The data were processed with Proteome Discoverer v. 1.2 (ThermoFisher Scientific) followed by a Mascot analysis (2.3.0; Matrix Science, Boston, MA) using the *Uniprot-Swissprot_mouse* protein database (05302013, 540261 protein sequences). Only proteins with at least two peptides (false positive discovery rate ≤ 1%) in one of the two samples were retained. Two independent pulldowns were used for MS and proteomic analysis. The proteins were analyzed with String-Db to categorize them based on their biological processes (17).

siRNA-mediated knockdown, RNA isolation, and quantitative PCR

3T3-L1 cells were seeded at a density of 75,000/well prior to transfection with control siRNA or two independent target-specific Silencer Select siRNA 1 or 2 (ThermoFisher Scientific). Transfection was performed using Lipofectamine RNAimax, as per manufacturer instructions (ThermoFisher Scientific), at a final siRNA concentration of 20 μM per well. Total RNA was isolated from 3T3-L1 adipocytes or MEFs with the RNEasy kit (Qiagen, Mississauga, Canada). Synthesis of cDNA was performed with the qScript cDNA Synthesis kit (Quanta Biosciences, Gaithersburg, MD), and transcript levels were measured with SYBR green chemistry or TaqMan assays on a QuantStudio 6-flex real-time PCR system (ThermoFisher Scientific). All data were normalized to *Hprt* by the $2^{-\Delta Ct}$ method, as previously described (4, 9, 35). All sequences of primers, TaqMan assays, and siRNAs can be found in Table S1. Confirmation that 14-3-3ζ knockdown had no effect of global RNA transcription was determined using the Click-iT RNA Alexa 488 imaging kit, as per the manufacturer's instructions (ThermoFisher Scientific).

Analysis of differential exon usage

To understand how adipocyte differentiation and depletion of 14-3-3ζ affected alternative splicing of mRNA, differential exon usage via DEXSeq was used as a surrogate measurement (30). Our previous transcriptomic data (GEO accession code GSE60745) were aligned to the mouse genome (Ensembl NCBIM37) via Tophat (v. 2.1.1). The number of reads mapping to a particular exon were compared with the total number of exons in a given gene and expressed as fragments per kilobase

per million mapped reads (30). A false discovery rate of 0.05 was used to filter results. This data set was also analyzed to examined how depletion of 14-3-3ζ or differentiation affects the expression profile of target genes. Genes identified by DEXSeq were subjected to gene ontology analysis to categorize genes by biological function (53). Analysis of *Lpin1* splicing was performed by RT-PCR, as described previously (32). PCR products were resolved on an agarose gel, followed by densitometric analysis of splice variants by ImageJ (31). Analysis of *Pparg* splicing was measured by quantitative PCR, using previously reported primer sequences against *Pparg1*, *Pparg2*, and *Pparg1sv* (29).

Immunoblotting

The cells were lysed in radioimmune precipitation assay (RIPA) buffer, supplemented with protease and phosphatase inhibitors, as previously described (4). Immunoprecipitation was performed on whole cell lysates from 3T3-L1 adipocytes at different stages of differentiation with established protocols (35). Proteins were resolved by SDS-PAGE, transferred to PVDF membranes, and probed with antibodies against 14-3-3ζ, Pparγ, Lipin-1, and β-actin (Cell Signaling Technology, Danvers, MA).

Statistical analysis

All data were analyzed by one- or two-way analysis of variance, followed by appropriate post hoc tests or by Student's *t* test. The data were considered significant when $p < 0.05$ and when applicable displayed as means ± S.D.

Author contributions—Y. M. performed experiments, analyzed data, and wrote and reviewed the manuscript. M. S. and N. N. F. performed experiments and analyzed data. T. M. designed parts of the study and reviewed the manuscript. G. E. L. performed experiments, analyzed data, wrote the manuscript, and is responsible for the integrity of this work.

Acknowledgments—We thank François Harvey in the Bioinformatics platform at the Centre Hospitalier de l'Université de Montréal for bioinformatics support and Dr. James D. Johnson (University of British Columbia, Vancouver, Canada) for critical reading of this manuscript.

References

1. Rosen, E. D., and MacDougald, O. A. (2006) Adipocyte differentiation from the inside out. *Nat. Rev. Mol. Cell Biol.* **7,** 885–896 CrossRef Medline
2. Cristancho, A. G., and Lazar, M. A. (2011) Forming functional fat: a growing understanding of adipocyte differentiation. *Nat. Rev. Mol. Cell Biol.* **12,** 722–734 CrossRef Medline
3. Scott, J. D., and Pawson, T. (2009) Cell signaling in space and time: where proteins come together and when they're apart. *Science* **326,** 1220–1224 CrossRef Medline
4. Lim, G. E., Albrecht, T., Piske, M., Sarai, K., Lee, J. T., Ramshaw, H. S., Sinha, S., Guthridge, M. A., Acker-Palmer, A., Lopez, A. F., Clee, S. M., Nislow, C., and Johnson, J. D. (2015) 14-3-3ζ coordinates adipogenesis of visceral fat. *Nat. Commun.* **6,** 7671 CrossRef Medline
5. Brunet, A., Kanai, F., Stehn, J., Xu, J., Sarbassova, D., Frangioni, J. V., Dalal, S. N., DeCaprio, J. A., Greenberg, M. E., and Yaffe, M. B. (2002) 14-3-3 transits to the nucleus and participates in dynamic nucleocytoplasmic transport. *J. Cell Biol.* **156,** 817–828 CrossRef Medline
6. Feige, J. N., and Auwerx, J. (2007) Transcriptional coregulators in the control of energy homeostasis. *Trends Cell Biol.* **17,** 292–301 CrossRef Medline
7. Nakae, J., Kitamura, T., Kitamura, Y., Biggs, W. H., 3rd, Arden, K. C., and Accili, D. (2003) The forkhead transcription factor Foxo1 regulates adipocyte differentiation. *Dev. Cell* **4,** 119–129 CrossRef Medline
8. Lim, G. E., and Johnson, J. D. (2016) 14-3-3zeta: A numbers game in adipocyte function? *Adipocyte* **5,** 232–237 CrossRef Medline
9. Lim, G. E., Piske, M., Lulo, J. E., Ramshaw, H. S., Lopez, A. F., and Johnson, J. D. (2016) Ywhaz/14-3-3ζ deletion improves glucose tolerance through a GLP-1-dependent mechanism. *Endocrinology* **157,** 2649–2659 CrossRef Medline
10. Pozuelo Rubio, M., Geraghty, K. M., Wong, B. H., Wood, N. T., Campbell, D. G., Morrice, N., and Mackintosh, C. (2004) 14-3-3-affinity purification of over 200 human phosphoproteins reveals new links to regulation of cellular metabolism, proliferation and trafficking. *Biochem. J.* **379,** 395–408 CrossRef Medline
11. Chen, S., Synowsky, S., Tinti, M., and MacKintosh, C. (2011) The capture of phosphoproteins by 14-3-3 proteins mediates actions of insulin. *Trends Endocrinol. Metab.* **22,** 429–436 CrossRef Medline
12. Siersbæk, R., Nielsen, R., John, S., Sung, M. H., Baek, S., Loft, A., Hager, G. L., and Mandrup, S. (2011) Extensive chromatin remodelling and establishment of transcription factor "hotspots" during early adipogenesis. *EMBO J.* **30,** 1459–1472 CrossRef Medline
13. Siersbæk, R., Rabiee, A., Nielsen, R., Sidoli, S., Traynor, S., Loft, A., Poulsen, L. C., Rogowska-Wrzesinska, A., Jensen, O. N., and Mandrup, S. (2014) Transcription factor cooperativity in early adipogenic hotspots and super-enhancers. *Cell Rep.* **7,** 1443–1455 CrossRef Medline
14. Johnson, C., Tinti, M., Wood, N. T., Campbell, D. G., Toth, R., Dubois, F., Geraghty, K. M., Wong, B. H., Brown, L. J., Tyler, J., Gernez, A., Chen, S., Synowsky, S., and MacKintosh, C. (2011) Visualization and biochemical analyses of the emerging mammalian 14-3-3-phosphoproteome. *Mol. Cell Proteomics* **10,** M110.005751
15. Mackintosh, C. (2004) Dynamic interactions between 14-3-3 proteins and phosphoproteins regulate diverse cellular processes. *Biochem. J.* **381,** 329–342 CrossRef Medline
16. Li, Y. (2010) Commonly used tag combinations for tandem affinity purification. *Biotechnol. Appl. Biochem.* **55,** 73–83 CrossRef Medline
17. Szklarczyk, D., Morris, J. H., Cook, H., Kuhn, M., Wyder, S., Simonovic, M., Santos, A., Doncheva, N. T., Roth, A., Bork, P., Jensen, L. J., and von Mering, C. (2017) The STRING database in 2017: quality-controlled protein-protein association networks, made broadly accessible. *Nucleic Acids Res.* **45,** D362–D368 CrossRef Medline
18. Liu, D., Lin, Y., Kang, T., Huang, B., Xu, W., Garcia-Barrio, M., Olatinwo, M., Matthews, R., Chen, Y. E., and Thompson, W. E. (2012) Mitochondrial dysfunction and adipogenic reduction by prohibitin silencing in 3T3-L1 cells. *PLoS One* **7,** e34315 CrossRef Medline
19. Ande, S. R., Nguyen, K. H., Padilla-Meier, G. P., Wahida, W., Nyomba, B. L., and Mishra, S. (2014) Prohibitin overexpression in adipocytes induces mitochondrial biogenesis, leads to obesity development, and affects glucose homeostasis in a sex-specific manner. *Diabetes* **63,** 3734–3741 Medline
20. Ding, S. Y., Lee, M. J., Summer, R., Liu, L., Fried, S. K., and Pilch, P. F. (2014) Pleiotropic effects of cavin-1 deficiency on lipid metabolism. *J. Biol. Chem.* **289,** 8473–8483 CrossRef Medline
21. Perez-Diaz, S., Johnson, L. A., DeKroon, R. M., Moreno-Navarrete, J. M., Alzate, O., Fernandez-Real, J. M., Maeda, N., and Arbones-Mainar, J. M. (2014) Polymerase I and transcript release factor (PTRF) regulates adipocyte differentiation and determines adipose tissue expandability. *FASEB J.* **28,** 3769–3779 CrossRef Medline
22. McLennan, Y., Polussa, J., Tassone, F., and Hagerman, R. (2011) Fragile x syndrome. *Curr. Genomics* **12,** 216–224 CrossRef Medline
23. Brasaemle, D. L., Dolios, G., Shapiro, L., and Wang, R. (2004) Proteomic analysis of proteins associated with lipid droplets of basal and lipolytically stimulated 3T3-L1 adipocytes. *J. Biol. Chem.* **279,** 46835–46842 CrossRef Medline

24. Wahl, M. C., Will, C. L., and Lührmann, R. (2009) The spliceosome: design principles of a dynamic RNP machine. *Cell* **136,** 701–718 CrossRef Medline
25. Pawellek, A., McElroy, S., Samatov, T., Mitchell, L., Woodland, A., Ryder, U., Gray, D., Lührmann, R., and Lamond, A. I. (2014) Identification of small molecule inhibitors of pre-mRNA splicing. *J. Biol. Chem.* **289,** 34683–34698 CrossRef Medline
26. Zhu, Y., Qi, C., Korenberg, J. R., Chen, X. N., Noya, D., Rao, M. S., and Reddy, J. K. (1995) Structural organization of mouse peroxisome proliferator-activated receptor γ (mPPAR γ) gene: alternative promoter use and different splicing yield two mPPARγ isoforms. *Proc. Natl. Acad. Sci. U.S.A.* **92,** 7921–7925 CrossRef Medline
27. Tontonoz, P., Hu, E., Graves, R. A., Budavari, A. I., and Spiegelman, B. M. (1994) mPPARγ2: tissue-specific regulator of an adipocyte enhancer. *Genes Dev.* **8,** 1224–1234 CrossRef Medline
28. Fajas, L., Auboeuf, D., Raspé, E., Schoonjans, K., Lefebvre, A. M., Saladin, R., Najib, J., Laville, M., Fruchart, J. C., Deeb, S., Vidal-Puig, A., Flier, J., Briggs, M. R., Staels, B., Vidal, H., *et al.* (1997) The organization, promoter analysis, and expression of the human PPARγ gene. *J. Biol. Chem.* **272,** 18779–18789 CrossRef Medline
29. Takenaka, Y., Inoue, I., Nakano, T., Shinoda, Y., Ikeda, M., Awata, T., and Katayama, S. (2013) A novel splicing variant of peroxisome proliferator-activated receptor-γ (Pparγ1sv) cooperatively regulates adipocyte differentiation with Pparγ2. *PLoS One* **8,** e65583 CrossRef Medline
30. Anders, S., Reyes, A., and Huber, W. (2012) Detecting differential usage of exons from RNA-seq data. *Genome Res.* **22,** 2008–2017 CrossRef Medline
31. Schneider, C. A., Rasband, W. S., and Eliceiri, K. W. (2012) NIH Image to ImageJ: 25 years of image analysis. *Nat. Methods* **9,** 671–675 CrossRef Medline
32. Péterfy, M., Phan, J., and Reue, K. (2005) Alternatively spliced lipin isoforms exhibit distinct expression pattern, subcellular localization, and role in adipogenesis. *J. Biol. Chem.* **280,** 32883–32889 CrossRef Medline
33. Li, H., Cheng, Y., Wu, W., Liu, Y., Wei, N., Feng, X., Xie, Z., and Feng, Y. (2014) SRSF10 regulates alternative splicing and is required for adipocyte differentiation. *Mol. Cell. Biol.* **34,** 2198–2207 CrossRef Medline
34. Vernia, S., Edwards, Y. J., Han, M. S., Cavanagh-Kyros, J., Barrett, T., Kim, J. K., and Davis, R. J. (2016) An alternative splicing program promotes adipose tissue thermogenesis. *eLife* **5,** e17672
35. Lim, G. E., Piske, M., and Johnson, J. D. (2013) 14-3-3 proteins are essential signalling hubs for beta cell survival. *Diabetologia* **56,** 825–837 CrossRef Medline
36. Knott, G. J., Bond, C. S., and Fox, A. H. (2016) The DBHS proteins SFPQ, NONO and PSPC1: a multipurpose molecular scaffold. *Nucleic Acids Res.* **44,** 3989–4004 CrossRef Medline
37. Kowalska, E., Ripperger, J. A., Hoegger, D. C., Bruegger, P., Buch, T., Birchler, T., Mueller, A., Albrecht, U., Contaldo, C., and Brown, S. A. (2013) NONO couples the circadian clock to the cell cycle. *Proc. Natl. Acad. Sci. U.S.A.* **110,** 1592–1599 CrossRef Medline
38. Wang, J., Rajbhandari, P., Damianov, A., Han, A., Sallam, T., Waki, H., Villanueva, C. J., Lee, S. D., Nielsen, R., Mandrup, S., Reue, K., Young, S. G., Whitelegge, J., Saez, E., Black, D. L., *et al.* (2017) RNA-binding protein PSPC1 promotes the differentiation-dependent nuclear export of adipocyte RNAs. *J. Clin. Invest.* **127,** 987–1004 CrossRef Medline
39. Li, S., Li, Z., Shu, F. J., Xiong, H., Phillips, A. C., and Dynan, W. S. (2014) Double-strand break repair deficiency in NONO knockout murine embryonic fibroblasts and compensation by spontaneous upregulation of the PSPC1 paralog. *Nucleic Acids Res.* **42,** 9771–9780 CrossRef Medline
40. Chaudhury, A., Chander, P., and Howe, P. H. (2010) Heterogeneous nuclear ribonucleoproteins (hnRNPs) in cellular processes: focus on hnRNP E1's multifunctional regulatory roles. *RNA* **16,** 1449–1462 CrossRef Medline
41. Dreyfuss, G., Kim, V. N., and Kataoka, N. (2002) Messenger-RNA-binding proteins and the messages they carry. *Nat. Rev. Mol. Cell Biol.* **3,** 195–205 CrossRef Medline
42. Nilsen, T. W., and Graveley, B. R. (2010) Expansion of the eukaryotic proteome by alternative splicing. *Nature* **463,** 457–463 CrossRef Medline
43. Lin, J. C. (2015) Impacts of alternative splicing events on the differentiation of adipocytes. *Int. J. Mol. Sci.* **16,** 22169–22189 CrossRef Medline
44. Mei, B., Zhao, L., Chen, L., and Sul, H. S. (2002) Only the large soluble form of preadipocyte factor-1 (Pref-1), but not the small soluble and membrane forms, inhibits adipocyte differentiation: role of alternative splicing. *Biochem. J.* **364,** 137–144 CrossRef Medline
45. Capobianco, V., Nardelli, C., Ferrigno, M., Iaffaldano, L., Pilone, V., Forestieri, P., Zambrano, N., and Sacchetti, L. (2012) miRNA and protein expression profiles of visceral adipose tissue reveal miR-141/YWHAG and miR-520e/RAB11A as two potential miRNA/protein target pairs associated with severe obesity. *J. Proteome Res.* **11,** 3358–3369 CrossRef Medline
46. Insenser, M., Montes-Nieto, R., Vilarrasa, N., Lecube, A., Simó, R., Vendrell, J., and Escobar-Morreale, H. F. (2012) A nontargeted proteomic approach to the study of visceral and subcutaneous adipose tissue in human obesity. *Mol. Cell Endocrinol.* **363,** 10–19 CrossRef Medline
47. Segerstolpe, Å., Palasantza, A., Eliasson, P., Andersson, E. M., Andréasson, A. C., Sun, X., Picelli, S., Sabirsh, A., Clausen, M., Bjursell, M. K., Smith, D. M., Kasper, M., Ämmälä, C., and Sandberg, R. (2016) Single-cell transcriptome profiling of human pancreatic islets in health and type 2 diabetes. *Cell Metab.* **24,** 593–607 CrossRef Medline
48. Tang, S., Bao, H., Zhang, Y., Yao, J., Yang, P., and Chen, X. (2013) 14-3-3ϵ mediates the cell fate decision-making pathways in response of hepatocellular carcinoma to Bleomycin-induced DNA damage. *PLoS One* **8,** e55268 CrossRef Medline
49. Benzinger, A., Muster, N., Koch, H. B., Yates, J. R., 3rd, Hermeking, H. (2005) Targeted proteomic analysis of 14-3-3 sigma, a p53 effector commonly silenced in cancer. *Mol. Cell Proteomics* **4,** 785–795 CrossRef Medline
50. Shevchenko, A., Chernushevich, I., Wilm, M., and Mann, M. (2000) *De novo* peptide sequencing by nanoelectrospray tandem mass spectrometry using triple quadrupole and quadrupole/time-of-flight instruments. *Methods Mol. Biol.* **146,** 1–16 Medline
51. Rappsilber, J., Mann, M., and Ishihama, Y. (2007) Protocol for micro-purification, enrichment, pre-fractionation and storage of peptides for proteomics using StageTips. *Nat. Protoc.* **2,** 1896–1906 CrossRef Medline
52. Ng, A. H., Fang, N. N., Comyn, S. A., Gsponer, J., and Mayor, T. (2013) System-wide analysis reveals intrinsically disordered proteins are prone to ubiquitylation after misfolding stress. *Mol. Cell Proteomics* **12,** 2456–2467 CrossRef Medline
53. Carbon, S., Ireland, A., Mungall, C. J., Shu, S., Marshall, B., Lewis, S., AmiGO Hub, and Web Presence Working Group (2009) AmiGO: online access to ontology and annotation data. *Bioinformatics* **25,** 288–289 CrossRef Medline